COMPDYN 2015
5th ECCOMAS Thematic Conference on
Computational Methods in Structural Dynamics and Earthquake Engineering
M. Papadrakakis, V. Papadopoulos, V. Plevris (eds.)
Crete Island, Greece, 25–27 May 2015

ESTIMATION OF CUMULATIVE SEISMIC DAMAGE TO URM BUILDINGS DURING EARTHQUAKE SEQUENCES

Amaryllis Mouyiannou[1], Maria Rota[1] and Andrea Penna[1,2]

[1] European Centre for Training and Research in Earthquake Engineering
Via Ferrata 1, I-27100 Pavia
amaryllis.mouyiannou@eucentre.it, maria.rota@eucentre.it

[2] Department of Civil Engineering and Architecture, University of Pavia
Via Ferrata 3, I-27100 Pavia
andrea.penna@unipv.it

Keywords: earthquake sequence, seismic demand, cumulative damage, unreinforced masonry buildings, SDOF models

Abstract. *During seismic sequences, repeated shocks of varying intensity hit previously damaged and unrepaired building stock. The cumulative damage from repeated shocks affects the building vulnerability to subsequent events. This paper introduces a methodology for estimating the displacement demand, assumed as a damage measure, to existing unreinforced masonry buildings during earthquake sequences in probabilistic terms, only given the intensity levels of each event of the sequence. The damage prediction is based on statistical interpretation of a collection of analytical results derived prior to the occurrence of the seismic sequence. This procedure can be a useful tool when a rapid evaluation of damage is desirable during the earthquake sequence, in order to be incorporated into risk and loss assessment calculations. The analytical results used for damage predictions consist of results of nonlinear dynamic analyses with a large number of unscaled records and a set of SDOF models representing undamaged and damaged URM buildings. In order to investigate the parameters that affect cumulative damage evaluation, application examples are developed by considering records from the Canterbury (New Zealand, 2010-2011) and the Emilia (Italy, 2012) earthquake sequences.*

1 INTRODUCTION

The undesired implications of cumulative damage on the seismic performance of unreinforced masonry buildings (URM) were recently observed during earthquake sequences that occurred in various locations (e.g. the demise of URM buildings after the Canterbury earthquake sequence, New Zealand, 2010-2011 [1][2] and Emilia, Italy, 2012 [3]). The need of developments in the quantification of aftershock risk calculation for pre-damaged buildings became obvious for all buildings, and especially URM buildings, since they constitute a large proportion of the total existing building stock, even in many seismically active countries. This paper proposes a procedure for calculating, in probabilistic terms, the expected seismic demand, by only knowing the intensity level of each earthquake event. This procedure uses the intensity levels of the events that have occurred (during a sequence), for the derivation of a distribution of demand values. Specifically, the procedure takes advantage of the results of state-dependent assessment (results of dynamic analyses performed with pre-damaged models and a large number of unscaled records), to proceed to a quick estimation of seismic demand during an earthquake sequence, without further analysis and by considering only the intensity of the occurring earthquakes and the damage state of the structures due to the preceding earthquake events.

The probabilistic prediction of damage demand for an earthquake sequence can be a useful tool for rapid post-earthquake assessment of a population of buildings, each represented by a model, whose seismic response can be evaluated by means of nonlinear time-history analyses (NLTHA) prior to the occurrence of the sequence. In particular, it can be very useful for emergency assessments, since a quick estimation of damage expectation is possible as soon as the sequence occurs. This could provide, very quickly, a basic idea for the decision-makers regarding the damage distribution among the building population, which was modelled and analyzed with dynamic analyses prior to the occurrence of the earthquake sequence. Moreover, the predictions referring to a single event can be combined with seismic hazard models, in order to derive the seismic risk and loss for expected earthquake events. Alternatively, during the occurrence of seismic sequences, the expected seismic demand can be combined with aftershock seismic hazard and the probability that seismic demand exceeds the limit states of interest can be calculated for given time ranges. Since aftershock hazard is time-dependent [4][5], the calculations can be repeated as the time lapses, by adopting the updated hazard or the updated demand, if more aftershocks are occurring. The outcome of each calculation can be interesting for stakeholders and decision makers for organizing emergency plans.

In the following sections, the methodology for the demand prediction is presented and some necessary considerations for obtaining a reliable prediction are discussed. Then, its applicability is examined through calculations of demand with four real earthquake sequences, for a single case study URM building.

2 OUTLINE OF THE PROPOSED METHODOLOGY

The procedure for deriving a probabilistic estimate of the expected displacement demand (and corresponding damage) for earthquake sequences can be divided in two parts, which will be discussed in the following sub-sections. The first and more time-consuming part should be performed prior to the occurrence of the sequence and includes the modelling and analyses in order to obtain maximum displacement (or other damage index) demand, as a function of the level of pre-existing damage and of the shock intensity, covering an adequate range of intensity measure (IM) values, consistent with the seismic hazard of the area. The second and quicker part (post-earthquake sequence) can be performed either by using the IM values of each event that has occurred during the sequence, in order to assess the accumulated damage,

or by using IM values of hypothetical sequences relevant to the aftershock seismic hazard at the site, in order to assess future demands. The distributions of the expected damage are then calculated for each shock. It should be noted that only the most significant records of the sequence should be used in the calculation. The exclusion of records of intensity below an adequate IM threshold is intended to exclude non-damaging earthquake events in order to speed up the damage prediction. The repetition of events of low intensity could indeed potentially change the expected response, depending on the model and the EDP used.

2.1 Calculation of displacement demand (before earthquake sequence)

The first steps of the procedure are common to those presented in [6], for the derivation of state-dependent fragility curves for URM buildings:

- Step 1: Derivation of appropriate multi-degree-of-freedom (MDOF) models representative of the building typologies of interest and calibration with adequate mechanical properties.
- Step 2 (Optional): Derivation of single-degree-of-freedom (SDOF) models, calibration and verification according to static and dynamic analyses with the MDOF models (if the response can be represented by SDOF models).
- Step 3: Derivation of pre-damaged models, representing the implications of damage experienced due to previous earthquake shocks on the building behavior during subsequent earthquake events, for example with a nonlinear static procedure (cyclic pushover analysis).
- Step 4: Selection of a sufficient number of appropriate records representative of the possible seismic action at the site of interest.
- Step 5: Calculation of seismic demand by means of NLTHA with the selected records and the undamaged and pre-damaged SDOF (or MDOF) models.
- Step 6: Representation of ground motions by appropriate scalar or low-order vector IMs.
- Step 7: Storing of analytical results, in terms of damage (displacement or drift) demands and the corresponding ground motion IM values, for each considered level of pre-existing damage.

2.2 Rapid evaluation of cumulative seismic damage (after earthquake sequence)

The steps to be carried out after the occurrence of a seismic sequence, in order to obtain a rapid evaluation of the cumulative damage consist of:

- Step 1: Representation of the earthquake sequence by a sequence of IM values.
- Step 2: Given the IM value of each earthquake event of the sequence, derivation of maximum displacement demand in probabilistic terms (using the results of the undamaged models for the first earthquake and by combining the results for damaged models for the rest of the events of the sequence). The final prediction regards the maximum damage demand that the building is expected to experience during the whole sequence.

The derivation of the distribution of maximum displacement demand is based on simple probability rules. For the first earthquake of the sequence, given its intensity, the displacement demand distribution (discrete levels) is taken from the previously calculated distributions of displacement from the results of NLTHA with the undamaged model, in a range in the vicinity of the IM value. The latter is based on the assumption that the building under examination is not damaged before the occurrence of the first strong motion of the studied sequence. According to the above, the probability of occurrence of discrete damage levels is

calculated $p(d_{\max,1} = DL_i \mid IM_{EQ1})$, where i corresponds to the damage levels (or bins) that have a non-zero probability of occurrence.

For the next considered earthquake event of the sequence, the probability of occurrence of each discrete damage level is calculated, according to the previously derived damage levels. Particularly, the probability that each damage level DL_j is reached after the second earthquake event is equal to the probability of DL_j, conditional on the pre-existing DL_i:

$$p(d_2 = DL_i \mid EQ_{1,2}) = \sum_{i=1}^{n_{DL}} p(d_{\max,2} = DL_j \mid IM_{EQ2} \mid d_{\max,1} = DL_i \mid IM_{EQ1}) \quad (1)$$

where n_{DL} represents the total number of damage levels (DLs) with non-zero probability of occurrence, during the previous earthquake events. Since the prediction focuses on the maximum experienced damage through the whole sequence, if the probabilistic calculation for the subsequent earthquake event includes damage levels lower than the lowest damage level reached at the preceding event, the probability of these low damage levels is added to the lowest damage level attained from the previous earthquake event.

For the subsequent earthquake of the sequence (3rd event), following the same principles as for calculating the damage demand for the sequence of EQ1 and EQ2, the probability of occurrence of each DL can be calculated according to:

$$p(d_3 = DL_k \mid EQ_{1,2,3}) = \sum_{i=1}^{n_{DL}} p(d_{\max,2} = DL_k \mid IM_{EQ3} \cap d_{\max,2} = DL_j \mid EQ_{1,2}) \quad (2)$$

In the same way, the probabilities of reaching each damage level are calculated for all the earthquakes of the considered sequence. Finally, the probabilistic predictions of damage demand can be compared to the deterministic results of real earthquake sequences derived from NLTHA with the earthquake sequence records.

3 REPRESENTATION OF SEISMIC DEMAND FOR UNDAMAGED AND PRE-DAMAGED MODELS

In this section, application examples of the procedure are presented in order to demonstrate its applicability and indicate the parameters that can affect the reliability of the probabilistic cumulative damage prediction. After a short presentation of the SDOF model used and the results of dynamic analysis (pre-earthquake steps), the probabilistic damage prediction calculations for four real earthquake sequences are presented and the considered parameters are introduced.

3.1 URM building model and considered levels of pre-existing damage

A model of a two-storey typical clay-brick URM building was used for the application examples. The building was assumed to develop a global in-plane failure mechanism, assuming that the out-of-plane failure of the walls is prevented. First, a MDOF model was developed using the software TREMURI [7][8], with mechanical properties adopted from ranges derived from collection and processing of available parameters for clay-brick masonry from experimental studies. Then, in order to reduce the computational burden of the necessary nonlinear dynamic analyses, an equivalent SDOF model was developed, according to the procedure proposed by Graziotti et al. [9], consisting of a static and dynamic calibration. The scheme adopted for the SDOF model is reported in Figure 1. The system is composed of two two-node macro-elements coupled by an axially rigid link, with the scope of allowing an accurate reproduction of the behaviour of the structure, characterised by a combination of flexural (left macro-element) and shear (right macro-element) responses. The degree of freedom corresponds to the horizontal displacement of the mass on top of the system. The

procedure followed for the calibration of the equivalent SDOF system is described in more detail in [6] and [9].

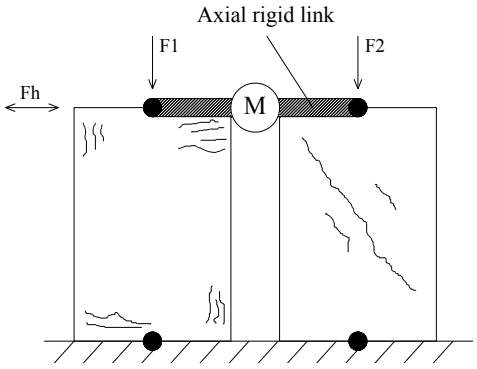

Figure 1: SDOF model of the selected building prototype [9].

This appropriately calibrated SDOF model was then used for the creation of models representing the various levels of pre-damage of the structure. For the applications presented here, the pre-damaged models were derived from the results of nonlinear static analysis, with reference to 15 discrete levels of damage, each represented by a level of top displacement of the MDOF model, starting from 2 mm (damage level 1, DL1) and increasing by 2 mm when moving to the following DL. In order to obtain the damaged model, the undamaged SDOF model was subjected to one loop of a cyclic pushover analysis up to the displacement level characterizing the damage level.

Alternative damage level definitions could obviously be adopted, depending on the application of the damage prediction. For example, the damage levels could correspond to significant damage states (DS), which would allow a direct calculation of loss when the DS are combined with corresponding loss values. Nevertheless, using damage levels independently defined from significant DS is preferred here because it does not require making assumptions on the definition of the limit states, whose uncertainty can have a strong impact on the procedure [10][11]. Lastly, the limit to the number of possible considered damage levels is also set by the need to derive bins with a reasonable number of NLTHA results for the derivation of damage distributions. For the application examples presented in the following, it was assumed that a more detailed discretization of DLs was not likely to be beneficial.

In order to be consistent, the maximum displacement used for deriving the pre-damaged models by cyclic pushover analyses should coincide with the displacement characterizing the *DLi* for the calculations of the post-earthquake assessment. A uniform definition of damage levels allows, during the calculation of seismic demand for sequences, to use results from analyses with pre-damaged model up to the displacement corresponding to *DLi*, if a model has reached *DLi* in a preceding record of the sequence. During all the steps of the procedure, the damage levels can be converted into displacement demand values and vice versa.

Finally, before applying the procedure for predicting the response during earthquake sequences, the maximum considered DL should be decided. Independently from the model used for NLTHA, either MDOF or SDOF, an upper threshold of displacement beyond which the structure is considered collapsed has to be set. For the following applications, a threshold of maximum MDOF displacement equal to 30 mm was selected and the results beyond 30 mm were considered as DL16, which can represent a collapse condition in the assessment scenarios.

3.2 Results of dynamic analyses

The relationships between displacement demand and ground motion intensity were derived from the results of NLTHA with the SDOF model and with the two horizontal components of the 467 real unscaled records of the SIMBAD database [12]. As already mentioned, meaningful intensity measures should be selected to characterise the severity of each accelerogram. For the applications of this paper, two scalar IMs and two two-dimensional vector-based IMs were considered. The aforementioned IMs were derived after a statistical investigation performed on the results of NLTHA, for a significant number of scalar and two-dimensional IMs [13]. In more detail, the selected scalar IMs were the Modified Housner Intensity, *mHI*, and the Average Spectral Acceleration, S_{aavg}, whereas the two vector IMs were composed by one of the aforementioned, as primary component, and the spectral shape factor, N_p [14], as secondary component. Housner Intensity is an energy-based intensity measure, calculated for each earthquake record as the integral of the pseudo-velocity spectrum (5% damping) for periods between 0.1 and 2.5 s [15]. This intensity measure was modified by reducing the period range of integration from 0.1 to 0.5 s (as already done in [9]), to better account for the period range of interest for masonry structures, whose effective fundamental period is rarely beyond 0.5s. Similarly, S_{aavg} was defined as the average of spectral acceleration for periods from 0 to 0.5s. Only combinations of the primary intensity measures with N_p were finally used, since N_p was found to be non-correlated to the primary components, whereas the opposite occurred for other secondary IMs examined (e.g. uniform duration [16] and peak ground acceleration).

Figure 2 shows the maximum displacement demand versus modified Housner Intensity values, obtained from NLTHA of the undamaged SDOF model with unscaled records from the SIMBAD database [12]. Since the number of records is decreasing for increasing intensity levels, the semi-logarithmic scale was used to allow a similar number of records in all the considered bins, in order to avoid giving different weights to the different bins. The green markers in the figure indicate the results considered for the maximum displacement prediction, while the rejected results, shown in red, correspond to values of displacement exceeding the maximum displacement limit (blue horizontal line) and maximum IM value (light blue vertical line). The IM upper limit was set as the level for which almost all the records lead to near collapse conditions (displacements higher than the collapse limit of 32 mm).

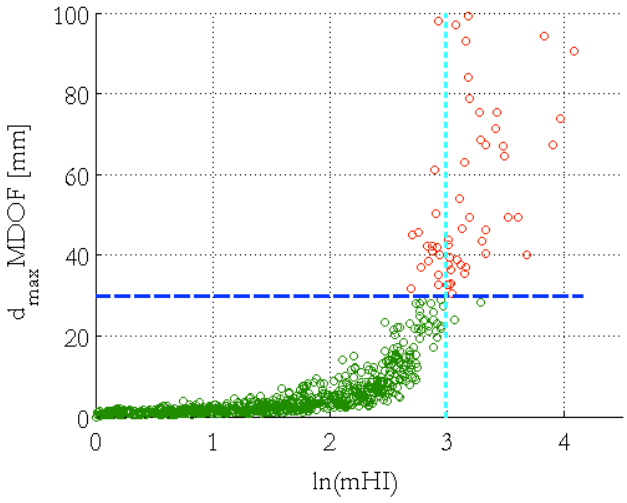

Figure 2 . Maximum displacement demand versus the logarithm of *mHI*

4 EXAMPLE OF QUICK PROBABILISTIC ESTIMATION OF DAMAGE DEMAND DURING A SEISMIC SEQUENCE

4.1 Considered real earthquake sequences

Four real earthquake sequences were considered for this example. The records of the first sequence were obtained from ITACA (Italian Accelerometric Archive, http://itaca.mi.ingv.it/) and were recorded at the Mirandola station (MRN) during the Emilia earthquake sequence in 2012. Additionally, the records of the three Christchurch sequences were obtained from GeoNet, (New Zealand geological database http://geonet.org.nz/) and correspond to the events of the Canterbury earthquake sequence that occurred in 2010-2012. The three considered stations are the Riccarton High School (RHSC), Papanui High School (PPHS) and Christchurch Hospital station (CHHC). A summary of the IM values of the ground motions of the considered sequences is provided in Table 1 and Table 2, for the NS components and EW components of the ground motions, respectively.

Station	Emilia (2012) MRN		Canterbury Earthquake Sequence (2010-2011) RHSC		PPHS		CHHC	
IM	*mHI* (m)	S_{aavg} (ms^{-2})	*mHI* (m)	S_{aavg} (ms^{-2})	*mHI* (m)	S_{aavg} (ms^{-2})	*mHI* (m)	S_{aavg} (ms^{-2})
EQ1	0.117	6.27	0.115	5.91	0.083	4.07	0.090	4.36
EQ2	0.086	4.91	0.145	7.13	0.102	4.89	0.188	8.81
EQ3	0.123	6.62	0.093	4.63	0.070	3.42	0.100	4.55
EQ4	0.056	3.34	0.114	5.87	0.095	4.53	0.090	4.36
EQ5	0.029	1.75	0.050	2.55	0.050	2.48	0.188	8.81
EQ6	-	-	0.094	4.93	0.062	2.90	0.077	4.03
EQ7	-	-	0.100	5.21	0.030	1.52	0.127	5.93
EQ8	-	-	0.090	4.54	0.045	2.25	0.100	4.55
EQ9	-	-	0.070	3.83	0.069	3.34	0.064	3.14
EQ10	-	-	-	-	-	-	0.079	3.86
EQ11	-	-	-	-	-	-	0.074	6.98

Table 1: Intensity measure values of the records of the considered sequences (NS components)

Station	MRN		RHSC		PPHS		CHHC	
IM	*mHI* (m)	S_{aavg} (ms^{-2})	*mHI* (m)	S_{aavg} (ms^{-2})	*mHI* (m)	S_{aavg} (ms^{-2})	*mHI* (m)	S_{aavg} (ms^{-2})
EQ1	0.140	7.11	0.100	5.05	0.088	4.47	0.075	3.56
EQ2	0.059	3.43	0.137	6.79	0.100	4.72	0.170	7.99
EQ3	0.095	5.41	0.152	7.49	0.097	4.59	0.067	3.43
EQ4	0.036	2.35	0.121	6.21	0.102	4.94	0.075	3.56
EQ5	0.043	2.97	0.038	2.08	0.061	2.86	0.170	7.99
EQ6	-	-	0.081	4.34	0.053	2.54	0.049	2.55
EQ7	-	-	0.083	4.41	0.047	2.32	0.065	3.18
EQ8	-	-	0.067	3.52	0.048	2.36	0.067	3.43
EQ9	-	-	0.070	3.75	0.051	2.52	0.055	2.74
EQ10	-	-	-	-	-	-	0.087	4.22
EQ11	-	-	-	-	-	-	0.0903	4.45

Table 2: Intensity measure values of the records of the considered sequences (EW components)

For the application examples presented here, only the events with at least one of the two components with *mHI* equal to or greater than 0.04 m were considered in the prediction calculations. It is worth highlighting (as can be seen from *mHI* values of the records of each sequence) that two moderate intensity sequences of ground motions were considered (recorded at RHSC and MRN), one low intensity sequence (recorded at PPHS) and one high intensity sequence (recorded at CHHC).

The displacement demand of each event and each entire sequence was calculated by NLTHA, in order to provide a measure of comparison to the median prediction of the damage demand, derived from the application of the methodology.

4.2 Evaluation of damage demand with earthquake events represented by scalar IMs

The calculation of cumulative damage demand was carried out for the four considered sequences of records. For each event, only the results from NLTHA with ground motions of IM values close to the IM value of the event were considered for the probabilistic calculation of damage levels. The IM range of interest was centred on the IM value of the considered event, whereas its width was defined taking into account the availability of high intensity ground motions in the adopted accelerometric database. Indeed, even for the highest level of ground motion, the number of records should be sufficient to allow the statistical treatment of the NLTHA results and the derivation of a displacement distribution.

For the presented results, the higher limit of the IM range was set equal to 0.20 m in terms of *mHI* and equal to 10 ms^{-2}, in terms of S_{aavg} and the IM range was divided into 10 bins. The resulting distribution of expected damage levels derived from the results of the undamaged model is shown in Figure 3 (top).

On the other hand, the ranges of the vector-based IMs were defined from adequate ranges of both components of the vectors. Primarily, the range of considered *mHI* or S_{aavg} values was derived and then, from the results contained in the range, only the results with values of N_p around the N_p value of the event were considered for the derivation of the damage distribution. The range of considered spectral shape ratio values was centred on the N_p value of the examined earthquake of the sequence (N_{PE}), plus and minus a fixed deviation of 0.15. It was observed that the deviation was not a governing parameter for the predictions. The limitation was set in order for the range of the second IM to be broad enough to include an adequate number of results for statistical use.

For each subsequent event, values of damage demand were calculated for all the levels of pre-existing damage, as indicated in the two multi-plots of Figure 3, for the two subsequent events of the MRN sequence.

Once the results were sorted in bins of IM and DL, the probabilistic displacement demand after each subsequent event was calculated, as well as the intermediate and final damage demand distributions, as shown in Figure 4 for the sequence recorded at MRN station.

The resulting damage levels for the complete sequences recorded in the four stations under study (components in the two perpendicular directions) are summarized in Figure 5 and Table 3. In Figure 5, each plot contains, for each direction, the median of the predicted damage demand for the sequences, represented either by the scalar *mHI* or S_{aavg}, or by considering them as primary components of vector-based IMs, combined to N_p. The deterministic demand derived from NLTHA with the time histories of the earthquake sequences is also included in the plots.

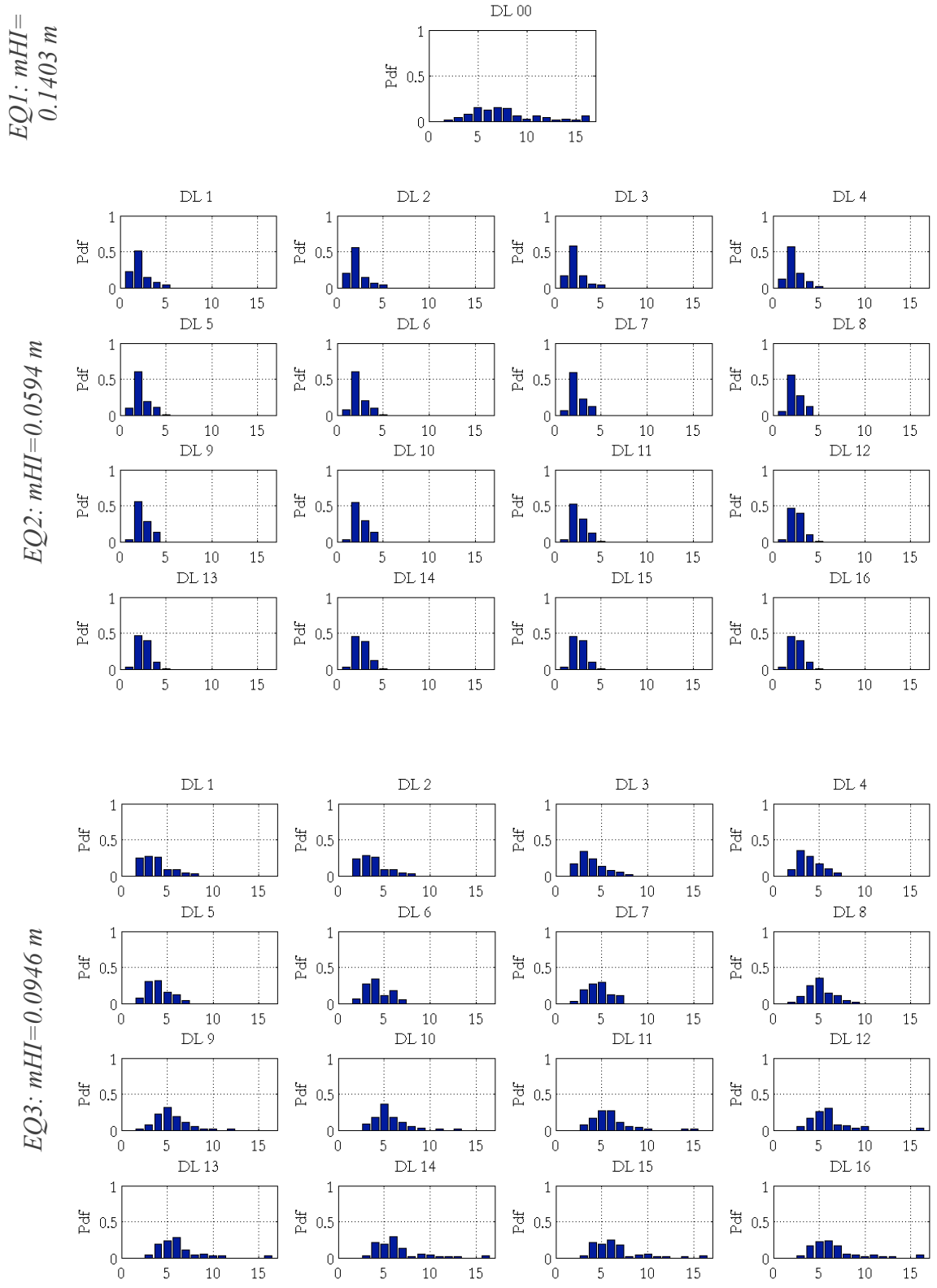

Figure 3: Predicted damage levels, for the undamaged model corresponding to the first earthquake event (top, EQ1) and for increasing levels of pre-existing damage (from DL1, top left, to DL16, bottom right), for the two subsequent events of the MRN sequence (EQ2 and EQ3)

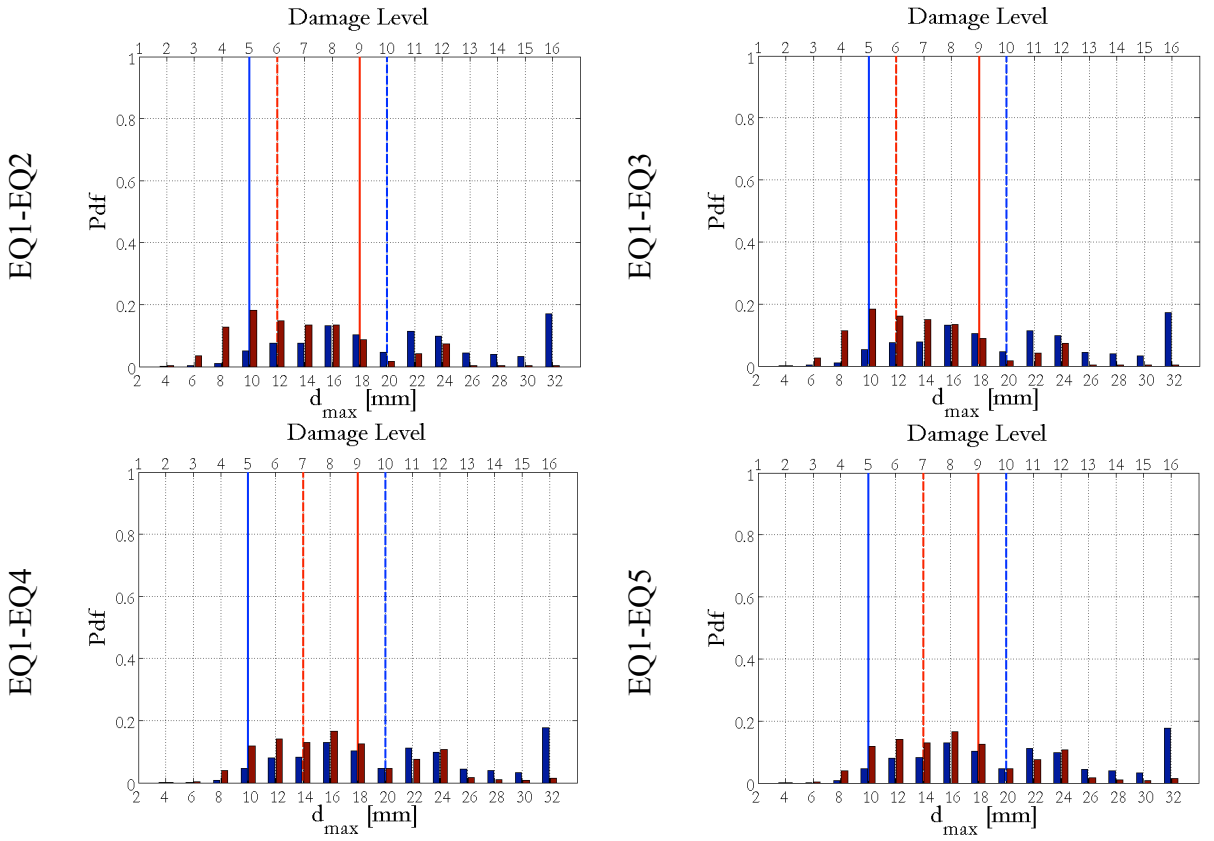

Figure 4: Probabilistic evaluation of seismic damage demand for subsequent events during an earthquake sequence (example of prediction with EW (blue) and NS (red) component of records from MRN station). The median values and the deterministic values for each component are indicated with dashed and continuous vertical lines, respectively, with the corresponding colour.

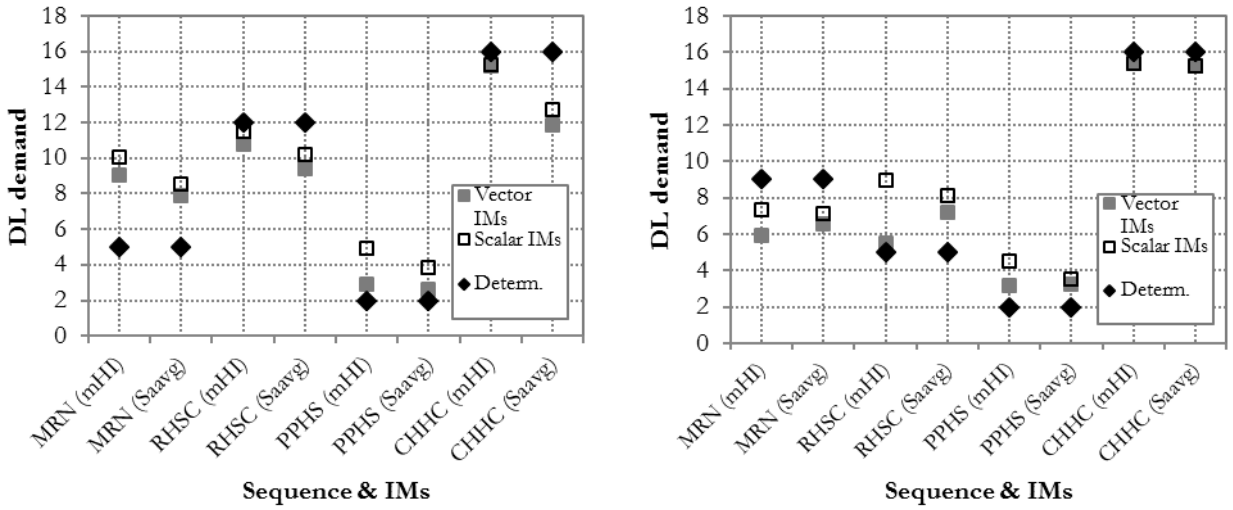

Figure 5: Median predicted damage levels for EW (left) and NS (right) components of the sequences recorded at MRN, RHSC, PPHS and CHHC. The deterministic response is indicated with black points. Each sequence is represented either with scalar IMs (ln(*mHI*) and ln(S_{aavg})) or vector IMs (ln(*mHI*)&Np and ln(S_{aavg})&Np)

The median values of the predicted maximum displacement distributions are found to be slightly lower than the deterministic response for the sequence recorded at the CHHC site (high intensity sequence), while the opposite is observed for the sequence recorded at PPHS (characterized by lower intensities). For the former case, the median of the prediction with *mHI* is closer to the deterministic results than the median of the prediction with S_{aavg} and the use of vector IMs instead of scalar ones does not seem to improve the median prediction. Conversely, for the latter case, prediction with S_{aavg} is closer to deterministic results and the use of vector IMs leads to median predictions closer to the deterministic results than the prediction calculated with scalar IMs. For the remaining sequence examples (recorded at RHSC and MRN), the deterministic response differs significantly between the two components of motion. It can be observed that, for the higher levels of damage, the use of *mHI* in the calculations leads to median values closer to the deterministic result. For the lower levels of damage (DL5), there is an overestimation of damage resulting from both the IMs (NS component of RHSC and EW component of MRN), which is slightly improved by using S_{aavg}. Still, with exception of RHSC (NS component), the use of vector IMs does not significantly affect the median prediction.

The precision of the predicted damage distributions can be evaluated by the scatter of the obtained probability distributions. If the results are assumed to follow a lognormal distribution, this scatter can be defined for example by the standard deviation of the lognormal distribution fitting them. More specifically, lognormal standard deviations can be calculated as one half of the difference of the logarithms of the displacement corresponding to the 84th percentile of the lognormal distribution and the one corresponding to the 16th percentile of the same distribution. The values calculated for all the sequences are shown in Table 3.

In the case of vector IMs, the damage distributions were found to be sensitive to the range of the considered primary IM and to the selected number of bins, especially for the earthquake sequences of moderate intensity (RHSC and MRN). For this reason, Table 3 reports lognormal standard deviation values corresponding to the cases of subdivision of the range of the primary IM both into 10 bins and 6 bins. The shaded cells indicate the lower values for each damage prediction.

	EQ seq.	*Scalar IMs(10bins)*		*Vector IMs(10binsIM1)*		*Vector IMs(6binsIM1)*	
		mHI	S_{aavg}	$mHI\&N_p$	$S_{aavg}\&N_p$	$mHI\&N_p$	$S_{aavg}\&N_p$
NS	*MRN*	0.42	0.44	0.49	0.46	0.52	0.52
	RHSC	0.33	0.40	0.44	0.48	0.55	0.59
	PPHS	0.26	0.22	0.27	0.10	0.35	0.26
	CHHC	0.14	0.32	0.39	0.33	0.19	0.39
EW	*MRN*	0.36	0.39	0.38	0.37	0.48	0.46
	RHSC	0.39	0.39	0.47	0.47	0.47	0.45
	PPHS	0.29	0.28	0.32	0.30	0.34	0.27
	CHHC	0.02	0.14	0.19	0.14	0.03	0.19

Table 3: Lognormal standard deviations of the predicted damage distributions for the four considered earthquake sequences, for the cases of vector and scalar IMs

Table 3 shows that the predictions for moderate intensity sequences leads to large standard deviations for both scalar and vector IMs. By comparing the scatter of the predictions calculated with the two scalar IMs, it seems that the use of *mHI* leads to a slightly lower scatter for the majority of the sequences. For some cases, the scatter calculated with vector IMs was smaller than the scatter resulting from scalar IMs. An example is the case of S_{aavg} and N_p for the low intensity sequence (PPHS).
Nevertheless, given the sensitivity of the scatter to the number of bins used to divide the range of the primary IM, it seems that, for the cases considered in this study, the use of combinations of IMs does not provide a significant improvement over the use of a scalar IM.

4.3 Comparison between main-shock and complete sequence damage demand predictions

In its established form, the calculation of seismic risk is based on the vulnerability of buildings to a single earthquake, i.e. it does not account for the cumulative damage occurring to the buildings for subsequent events. Adversely, as observed during the occurrence of real earthquake sequences, the damage demand due to the main-shock only can be different from the damage demand due to the whole sequence. In this work, the potential differences between the prediction for the main-shocks only and for the entire sequence were investigated.

Figure 6 shows the damage predictions derived for the four investigated sequences, including the results from analyses with both components of earthquake motion, considering S_{aavg} as scalar IM. The damage levels derived from dynamic analyses with the records of the main event and the complete sequence are also reported in the plots, indicated with vertical continuous lines. It is noted that the event with the larger moment magnitude of each sequence was considered as the main-shock, even if the records at the considered stations did not have the largest local intensity value.

With the only exception of the sequence recorded at the PPHS station, considering the complete sequence increases the probability of higher levels of damage with respect to the case of the main-shock only. It is interesting to note that, for the sequence recorded at the MRN station, there is no increase in the damage demand with respect to that obtained from the deterministic values.

This comparison confirms that the use of the median value only of the predicted damage distributions should be avoided, and the scatter in the demand should always be accounted for.

For the majority of the main-shock predictions (with the only exception of the CHHC sequence), the demand distribution obtained for discrete levels of damage could be fitted with a lognormal distribution. This would allow the prediction calculation in a continuous range of damage and the development of a closed-form calculation of the damage demand, when the maximum value of earthquake intensity is known for a main-shock. Nevertheless, from the distributions resulting after damage calculations for complete sequences of events, it seems that the fitting by a mathematical distribution is not a trivial issue.

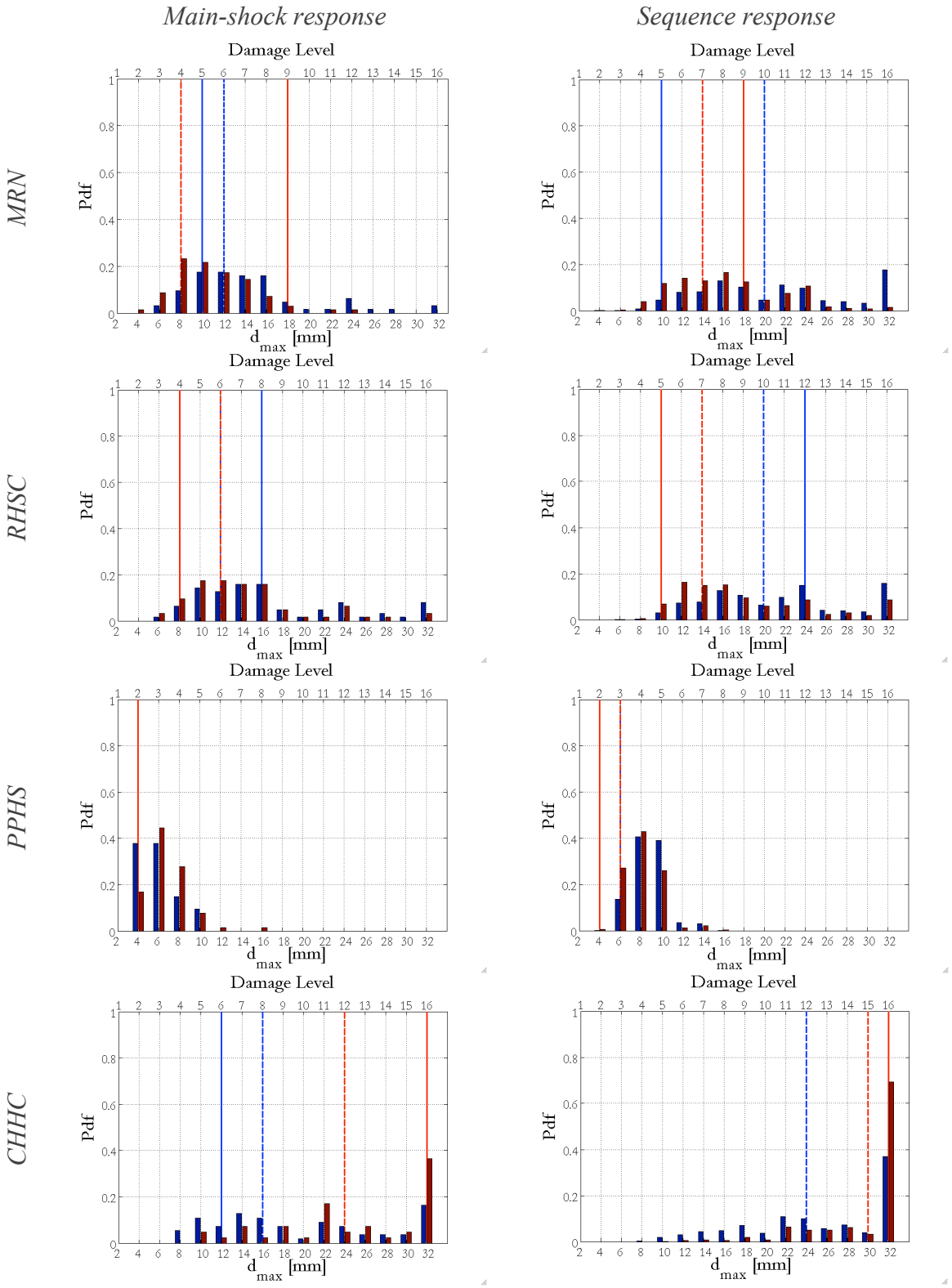

Figure 6: Predicted damage level distributions for main-shock (left) and entire sequence (right) for the four considered earthquake sequences (top to bottom), with EW and NS indicated by blue and red, respectively. The median values and the deterministic values for each component are indicated with dashed and continuous lines, respectively, with the corresponding colour.

4.4 Example of application of the proposed methodology for post-earthquake damage assessment

In several countries worldwide, after the occurrence of an earthquake event, fast-tagging procedures are often applied together with site surveys, where structural engineers are called to quantify the aftershock vulnerability and risk, mainly based on visual inspections, and judge if each building can be reused (green tag), further inspected (yellow) or in danger of collapse (red) in case of aftershocks. The decision is made without any knowledge of the transition probability of the observed damage to collapse. Some guidelines for the quantification of aftershock risk were provided in the past for reinforced concrete buildings [17]. The procedure developed in this work can allow some rapid calculations of damage demand, from the results of previous analytical studies, based on the seismic response of the structures of interest and the intensity of the events of the occurring sequence. This can provide indications for stake-holders and decision makers for organizing fast-assessment plans and prioritizing the operations.

The results of a simple example of this type of fast calculation, based on the results of analyses with pre-damaged SDOF models, are presented in Table 4. The probability distributions were calculated as previously, for the case of only main-shocks and for all events of the considered earthquake sequences. The only additional step required is an adequate definition of the limit state thresholds or, in other words, the translation of DL to significant DS, represented by the tagging colours. For the example presented here, three LS can be considered, consisting of operational limit state (OLS), damage limitation limit state (DLS) and ultimate limit state (ULS). Consequently, four damage states (DS1<OLS, OLS<DS2<DLS, DLS<DS3<ULS, DS4>ULS) are identified. The LS displacement thresholds were defined as the attainment of the first yielding pier for OLS, the attainment of the maximum base shear for DLS and the drop of base shear to 80% of its maximum value for ULS [13].

In this example, the green tag damage state corresponds to damage levels up to OLS, the yellow tag to damage levels between OLS and DLS and the red to damage levels beyond DLS. Making reference to the DLs adopted in this study, DL6 corresponds to the threshold for the attainment of OLS, while DL10 to the attainment of DLS. After DL10 the structure shows a degrading response, with the ULS obtained for DL12. For this example, all damage levels beyond DL10 are considered as red-tagged damage state. Table 4 reports the probabilities of damage occurrence of the three significant damage states, for the four considered sequences, considering either only the main-shock or the entire sequence. It can be observed that the probability of more severe damage is increasing if the entire sequence is considered in the damage prediction calculation.

DL	RHSC		PPHS		CHHC		MRN	
	Main-shock	Sequence	Main.	Seq.	Main.	Seq.	Main.	Seq.
<DL6	0.40	0.05	0.99	0.97	0.16	0.02	0.60	0.24
DL6-DL10	0.50	0.55	0.01	0.03	0.24	0.14	0.32	0.50
>DL10	0.10	0.40	0	0	0.60	0.84	0.08	0.26

Table 4: Example of tagging estimation: probabilistic prediction of damage states for four earthquake sequences (recorded at RHSC, PPHS, CHHC and MRN), considering only main-shocks or entire sequence of events

5 CONCLUDING REMARKS

A methodology for quick estimation of maximum displacement demand during and after earthquake sequences was proposed. The methodology was applied to a single case-study building, with the aim of investigating its applicability and identifying the parameters that can affect the reliability of the damage predictions. In more detail, the ability of the procedure to estimate (in probabilistic terms) the damage demand due to main-shocks and complete sequences was studied by means of four examples with real earthquake sequences and the predictions were compared to the seismic demand calculated with (deterministic) NLTHA with the considered records.

It is recognized that improvements in the procedure can and should be considered. First of all, the proposed procedure currently accounts only for the global response of the buildings, assuming that early local failure modes are prevented. The consideration of local out-of-plane mechanisms should be incorporated as a future development. A further improvement of the methodology could be aiming at deriving predictions of damage demands representative of more general building typologies, represented by similar geometries and varying mechanical properties.

Another possible improvement regards the SDOF model and the representative engineering demand parameter used to recreate the URM seismic response during earthquake sequences. Indeed, an advanced (MDOF) modelling that accounts for out-of-plane failures and allows partial collapses can be significantly more efficient in the prediction of damage. Nevertheless, the downside of the advanced modelling is that the more complex it is, the more case-specific it becomes, and therefore it cannot be adopted in the assessment of a large population of buildings. A compromise between the level of detail in the modelling and its representativeness of a building population should always be considered, taking also into account the inevitable increase of computational time when detailed models are used.

Lastly, former studies (e.g. [18]) showed that, in addition to the ground motion intensities, aftershock ground motion features such as the frequency content and the strong motion duration can affect the post-main-shock response. These aspects should be investigated within the damage prediction procedure and their impact should be studied through applications with more real earthquake examples.

Finally, for the validation of the procedure, empirical data for the observed damage evolution during earthquake sequences should be considered in order to assist the identification of representative thresholds corresponding to significant damage states. The analytical limit state thresholds should be related to more observational damage data, provided that the considered models adequately represent the seismic behaviour of the structures.

REFERENCES

[1] I. Senaldi, G. Magenes, J. Ingham, Damage assessment of unreinforced stone masonry buildings after the 2010-2011 Canterbury earthquakes, *International Journal of Architectural Heritage* [in press], 2015, DOI: 10.1080/15583058.2013.840688.

[2] L. Moon, D. Dizhur, I. Senaldi, H. Derakhshan, M. Griffith, G. Magenes, J. Ingham, The demise of the URM building stock in Christchurch during the 2010/2011 Canterbury earthquake sequence, *Earthquake Spectra*, **30**, 1, 253-276, 2013.

[3] A. Penna, P. Morandi, M. Rota, C.F. Manzini, F. da Porto, G. Magenes, Performance of masonry buildings during the Emilia 2012 earthquake, *Bulletin of Earthquake Engineering*, **12**, 5, 2255–2273, 2015.

[4] B.A. Bradley, R.P. Dhakal, M.Cubrinovski, J.B. Mander, G.A. MacRae, Improved seismic hazard model with application to probabilistic seismic demand analysis, *Earthquake Engineering and Structural Dynamics*, **36**,14, 2211-2225, 2007.

[5] I. Iervolino, M. Giorgio, B. Polidoro, Sequence-based probabilistic seismic hazard analysis, *Bulletin of the Seismological Society of America*, **104**, 2, 1006-1012, 2014.

[6] A. Mouyiannou, A. Penna, M. Rota, F. Graziotti, G. Magenes, Implications of cumulated seismic damage on the seismic performance of unreinforced masonry buildings, *Bulletin of New Zealand society for Earthquake Engineering,* **47**, 2, 157-170, 2014.

[7] A. Penna, S. Lagomarsino, A. Galasco, A nonlinear macro-element model for the seismic analysis of masonry buildings, *Earthquake Engineering and Structural Dynamics*, **43**, 2, 159-179, 2014.

[8] S. Lagomarsino, A. Penna, A. Galasco, S. Cattari, TREMURI program: an equivalent frame model for the nonlinear seismic analysis of masonry buildings, *Engineering Structures*, **56**, 1787-1799, 2013.

[9] F. Graziotti, A. Penna, G. Magenes, Use of equivalent SDOF systems for the evaluation of displacement demand for masonry buildings, *Proceedings of VEESD 2013*, Vienna, Austria, August 28-30, 2013.

[10] A. Mouyiannou, M. Rota, A. Penna, G. Magenes, Identification of suitable limit states from nonlinear dynamic analyses of masonry structures, *Journal of Earthquake Engineering*, **18**, 2, 231 – 263, 2014.

[11] M. Rota, A. Penna, G. Magenes, A methodology for deriving analytical fragility curves for masonry buildings based on stochastic nonlinear analyses, *Engineering Structures*, **32**, 5, 1312-1323, 2010.

[12] C. Smerzini, C. Galasso, I. Iervolino, R. Paolucci, Ground motion record selection based on broadband spectral compatibility, *Earthquake Spectra*, DOI: 10.1193/052312EQS197M, 2015.

[13] A. Mouyiannou, *Implications of cumulative damage on the seismic vulnerability of masonry buildings*, PhD Thesis, IUSS Pavia, 2014.

[14] E. Bojorquez, I. Iervolino, Spectral shape proxies and nonlinear structural response, *Soil Dynamis and Earthquake Engineering,* **31**, 996-1008, 2011.

[15] G.W. Housner, Behavior of structures during earthquakes, *Journal of the Engineering Division*, ASCE, **85**, EM14, 109-129, 1959.

[16] S.K. Sarma, B.J. Casey, Duration of strong motion in earthquakes, *Proceedings of the 9th WCEE*, Tokyo, Japan, 1990.

[17] P. Bazzurro, C.A. Cornell, C. Menun, M. Motahari, Guidelines for seismic assessment of damaged buildings, *Proceedings of 13WCEE*, Vancouver, Canada, 2004.

[18] J. Ruiz-Garcia, Mainshock-aftershock ground motion features and their influence in building's seismic response, *Journal of Earthquake Engineering,* **16**, 5, 719-737, 2012.